Implementation of 1D Brinson model in 3D SMA specimens Influenced by stress concentration

M. Kamrani[1], H. Vahabi[2], A. Imenabadi[3]

[1]*M.Sc. Graduate Student, School of Mechanical Engineering, Faculty of Engineering,*
University of Isfahan, Isfahan, Iran,
[2]*M.Sc. Graduate Student, School of Mechanical Engineering, Faculty of Engineering,*
University of Tehran, Tehran, Iran,
[3]*M.Sc. Graduate Student, School of Metallurgy Engineering, Faculty of Engineering,*
University of Sharif, Tehran, Iran,

Abstract:- The application of small-size SMA components has grown rapidly in various industries over the last few years. Due to their complex nature, local constitutive models for those components have proven somehow impractical; whereas global models have been unable to take the stress concentration into consideration and hence cannot predict the nucleation and stress patterns accurately, especially in small samples. Moreover, FE analyses are impossible to conduct in cases where a large number of evaluations are required to design a suitable SMA sample. This paper proposes a new iterative method to accurately calculate the stress and martensitic volume fraction in samples with stress concentration using 1D Brinson model. The method is implemented in the form of a computer code which is then refined iteratively using FEM model which is validated based on experimental data. Final assessments show that the proposed method could predict the stress values accurately at negligible computational costs.

Keywords:- SMA wires, Brinson constitutive model, martensite volume fraction, FEM, Stress concentration, modification algorithm.

I. INTRODUCTION

Shape memory alloys are in great demand in various industries ranged from aerospace to biomechanics based on their particular behavior named "shape memory effect (SME)" and "pseudoelasticity (PE)". A great amount of attempts have been devoted to develop a comprehensive constitutive model for shape memory alloys since their discovery in 1940. Different one-dimensional models such as Auricchio [1], Tanaka [2] etc. introduced the "Martensie Volume Fraction" to accurately predict the martensitic transformation's procedure, as a basis for outstanding behavior of these materials. Brinson, first addressed the martensite volume fraction in two different respects, "due to stress" and "due to temperature"; hence he could successfully model the material behavior in various conditions and modes [3]. This model assumes that the nucleation and propagation of transformation fronts occurs simultaneously and are homogenous along the length of the sample which is the Brinson fundamental assumption as well as its often quoted drawback; since any stress concentration may cause a significant change in homogeneous stress pattern in the sample which leads the nucleation and phase transformation to start locally and in a specific point of the sample. Therefore, Brinson fundamental assumption of homogeneous behavior and thus simultaneous nucleation and propagation of phase transformation in the sample usually ends up with an accurate transformation prediction which is totally different from what happens in reality [Brinson [4], Shaw [5, 6], and Rahman [7]]. This inaccuracy would be more troublesome in case material homogeneousness decreases as stress concentration span increases which is common in small small-scale samples. Therefore, Brinson model would not be practical in small-scale SMA samples, especially employed in robotics and biomechanics industries, due to its considerable deficiency in predicting the effect of stress concentration on phase transformation.

A large number of investigations have been performed to understand the non-homogeneous behavior of the shape memory alloys. Shaw carried out some tensile tests on slab samples and realized that stress reduces in sample in time of nucleation [6]. Hence, he assumed that the nucleation start stress is higher than the stress required for propagation of transformation fronts along the sample. Shaw designed an especial test stand [8] and performed some tensile test on slab samples in different temperatures. Thereby he could accurately calculate the critical stresses, nucleation stress as well as propagation stress, in different temperatures. Finally, considering these critical stresses, he could precisely simulate the psuduelastic behavior of shape memory alloys, especially in low strain rates, based on Luder plasticity theory [9, 10]. Luder plasticity theory is developed based on the

fact that stress reduces as the material enters the plastic region [9, 10]. Shaw also simulated the effect of environmental conditions as well as material parameters [11]. Martensite volume fraction was not considered in Shaw model and thus transformation propagation was traced through the variations in strain of the sample. Azadi enhanced the Shaw's model based on editing the heat generation equation with respect to the martensite volume fraction effect [12]. Both Shaw and Azadi models are suitable for predicting the material behavior in low-strain rates. Shaw and Azadi employed a dent in the sample under tension to artificially simulate the effect of stress concentration near the grippers. Some other models proposed to predict the details of localized behavior of shape memory and propagation of phase transformation are largely nonlocal, developed based on the balance of energy in isothermal conditions [13, 14]. Generally austenite tends to transform into martensite due to its relatively higher energy level compared to that of the martensite. Martensite volume fraction is not taken into account in these nonlocal models developed based on Luder theory. Moreover, these models are valid just in psuduelastic mode due to the limited scope of work in Luder theory.

Although SMA wires are of more practical use, strip specimens have been focused in most experimental investigations since nucleation and propagation phenomena are relatively easier to be distinguished and monitored in strips. Shaw and Kyriakides [5] and Zhang et al. [15] covered SMA strips with a brittle film, detaches from the surface due to large strains, to track the nucleation process and propagation of transformation fronts.

Despite their capabilities in precisely predicting the material behavior, implementation of local models are rare due to their relatively complicated procedure in measuring the required material parameters; hence 1D models, especially Brinson, are generally the most practical ones. However, 1D models accuracy is extremely menaced by stress concentration at investigated zone.

A new method to revise the accuracy of Brinson model based on stress concentration is proposed in this research in which, maximum stress is considered in prediction of nucleation and metallurgic phase. Without the loss of generality, a case study adapted for this framework is a narrow wire under tension. Initiation of the nucleation and transformation due to the stress concentration near the grippers is a common characteristic feature in samples under tension in test stand. Shaw [5] revealed that local transformation in a constant temperature at zones adjacent to the grippers causes a considerable reduction in stress and thus local bearing load capacity at mentioned zone (Fig.1). Fig.1 depicts that stress growth continues to reach the transformation start stress (point A) and followed by a slight decline during the transformation until reaching the finish stress (point B). This local reduction in strength of wire in nucleated points, transfers a fraction of local peak stress of this zone to the adjacent un-nucleated areas which may expedite the nucleation there. Therefore, stress concentration and nucleation close to the grippers, results in a full transformation entire wire cross section.
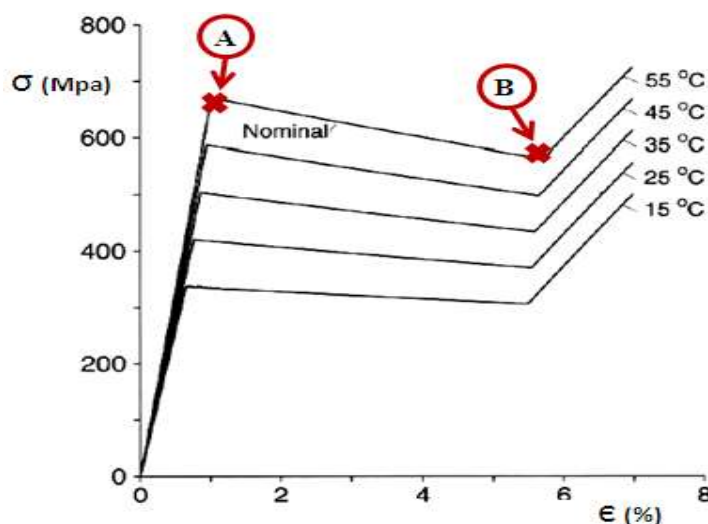

Fig.1. Transformation start (A) and ending (B) stresses in different temperatures, Shaw [5]

As mentioned, local nucleation in a cross section is unavoidable due to the increase in local stress near the grippers which is against the fundamental assumption of one-dimensional Brinson model. Hence Brinson model is unable to capture the local stress concentration and thus local nucleation due to the mentioned drawback.

The necessity to obtain more details from stress pattern and nucleation process in different operating modes to design an SMA sample accurately, has recently prompted the development of 3D numerical methods which do not invoke many simplifying assumptions. Finite element method (FEM), employing a number of

elements at cross section, can recognize the stress and thus probable nucleation in each element somehow independently. However, nonlinear analysis of SMA samples made up of SMA, especially when evaluation of various design parameters is needed, would be a time-consuming task. Furthermore, commercial FEM- based software is incapable of calculating the martensite volume fraction. Therefore, a FEM- based modification is proposed in this research to adequately calculate the stress distribution as well as nucleation and propagation along the sample.

Without loss of generality, an SMA wire was investigated to show the procedure of introduced modification method. To achieve that, a FE (finite element) model of the mentioned wire under tension was prepared and loaded sequentially. Stress distribution pattern along the sample, considering the stress concentration, were derived in some loading intervals. Following that, an iterative algorithm was developed to predict the maximum stress and thus martensite volume fraction in each section along the sample. The proposed algorithm employed stress patterns, extracted from the FE model, to recognize an initial stress pattern and revised the Brinson model based on maximum stress instead of mean stress at each section. The calibrated algorithm could be implemented in various load cases to accurately predict the maximum stress and thus nucleation and propagation of transformation fronts at each section along the sample. Therefore, a nonlinear, time consuming FE analysis is performed just once and all followed load cases are investigated using the mentioned code. Hence it results in more simple and more accurate design of SMA specimens via considering the stress concentration. Moreover, since this proposed code can be used with all constitutive models, it can be employed in different analyses such as fatigue and other isothermal hysteresis [16, 17, 18]. The developed code proved to be reliable according to a negligible difference between code and FE results.

II.   RESEARCH METHODOLOGY

A case study adopting for this framework was a small SMA wire under tension, with diameter and length of 1.5 and 100 mm, respectively which is very common in robotic, biomechanics etc. The wire was fixed at the bottom and its other end was pulled very slowly to prepare a quasi-static condition. The magnitude of stress concentration near grippers varies due to the grippers fastening load. Hence the lowest amount of grippers' load was employed to prevent sliding at interface between grippers and the sample. The supplied tension increased to an extend in which 7% strain was achieved which guaranteed a complete transformation along the entire length of the sample. Material properties of the wire are listed in table 1.

Table 1. Material properties of the wire												
parameter	T_{amb} (ºC)	ε_l	r (mm)	A_f (ºC)	A_s (ºC)	M_f (ºC)	M_s (ºC)	C_M (MpaK^{-1})	C_A (MpaK^{-1})	σ_{cr}^s (Mpa)	σ_{cr}^f (Mpa)	E_M (Gpa)	E_A (Gpa)
value	18	0.043	0.75	15	-1	-50	-45	6	5.6	20	80	16	**45**

As mentioned, the Brinson model is implemented in the developed code to recognize the stress pattern and martensite volume fraction along the sample. Martensite volume fraction is employed in Brinson model as an internal parameter to define the SMA behavior and predict the nucleation propagation pattern [3]

2.1.   Numerical model

Commercial FEM software was employed to derive the stress distribution along the sample which was implemented to calibrate the developed code. There were three symmetric planes in the sample, hence just a quarter part of the sample and grippers were modeled numerically (Fig.3) and normal displacements were fixed in all three symmetric planes. A higher-order brick element was applied to mesh the wire. Definition of a complex shape function would be possible due to 12 mid-nodes in the element which leads to a more accurate analysis. Being able to accurately capture the stress concentration near the head of the gripper, mesh was adjusted to be denser in this region (Fig.4). The gripper was assumed rigid and a surface to surface contact was defined between the gripper and sample faces. Furthermore, an employed master node for rigid surfaces of the gripper assisted us to define a unique boundary condition for them. All boundary conditions defined on the master node would automatically be distributed homogeneously on the gripper surfaces. A total number of 3200 elements were applied to prepare the mesh based on mesh study.
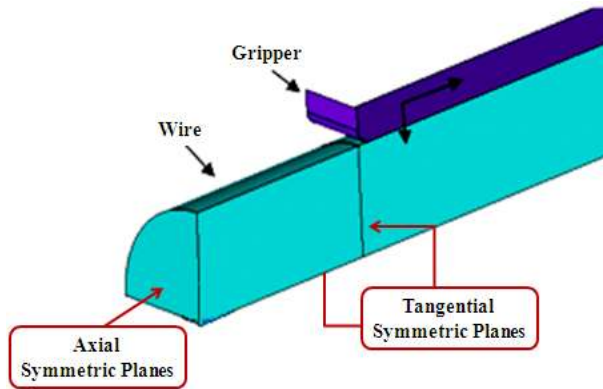
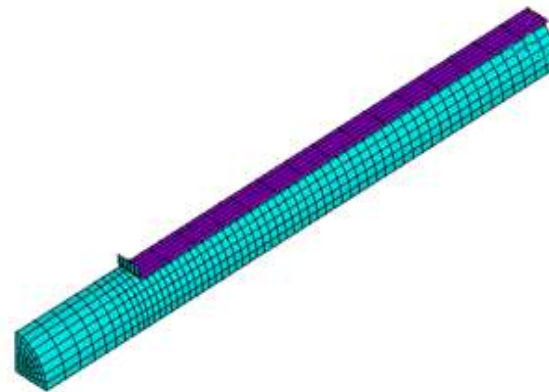**Fig.3. Geometry and boundary conditions used in numerical model**

Fig.4. Element size along the sample

An idealized SMA material model was implemented in FE model which its stress-strain diagram is depicted below. Fig.5 indicates that the SMA strength in linear elastic zone declines suddenly when it reaches the austenite transformation start stress (   ) and then recovers its strength as much, just as the tensile load passes the austenite transformation finish stress (   ). However, if the tensile load reduces again, the sample strength decreases in a totally different curve until reaching the martensite transformation start stress (   ) and continues to decline according to a different curve up to the martensite transformation finish stress (   ) which is followed by a strength recovery.
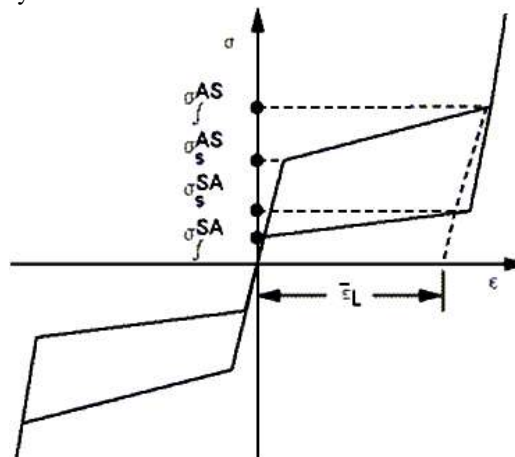

Fig.5. Idealized stress-strain curve in material model

All parameters used in idealized material model, mentioned in table.2, can be calculated based on material properties reported in table.1.

<table>
<tr><td colspan="7">Table 2. Idealized material properties of the sample</td></tr>
<tr><td>Parameter</td><td>r
(mm)</td><td>σ_f^{SA}
(Mpa)</td><td>σ_s^{SA}
(Mpa)</td><td>σ_s^{AS}
(Mpa)</td><td>σ_f^{AS}
(Mpa)</td><td>ε_l</td></tr>
<tr><td>Value</td><td>0.75</td><td>16.8</td><td>106.4</td><td>398</td><td>458</td><td>0.043</td></tr>
</table>

An often quoted drawback of this material model is that martensite volume fraction is not taken into account and just stress and strain pattern would be obtainable in FE models. A static analysis was performed in two sequential steps in displacement-control modes, in which the gripper initial compression was modeled in the first step and the tension of the sample was modeled in the second one. A considerable axial displacement was defined on master node of the gripper 1n the second step and the resultant strain was monitored.

2.2. Validation

To investigate the accuracy of numerical model, a tensile test was performed on an SMA wire with length of 120 mm and diameter of 1.5 mm. Engineering strain of the sample was monitored during the second step of loading to be employed in stress calculation based on Brinson model. The wire was long enough that effects of stress concentration near grippers disappear along the sample and could not influence the stress pattern in mid-span section. Therefore, Brinson model could accurately predict the stress in mid-span section based on the engineering strain in the wire.

A FE model of the tested sample was prepared and its nominal stress and engineering strain were calculated during the second load step using Eq.1 and Eq.2 below. All meshing requirements, material model, boundary conditions, etc. were identical to what mentioned in previous section.

$$Engineering\ S \qquad\qquad\qquad \text{Eq 1}$$

$$Nominal\ Stress = \frac{?}{\frac{?}{4}*cross\ sectic} \qquad\qquad \text{Eq 2}$$

Where *"Axial displacement"* is the exerted displacement on master node of the gripper and *"Axial force"* is the total axial load observed in the mid-span cross section of the sample.

"Nominal stress"-"engineering strain" curves extracted from numerical and Brinson-based experimental models are depicted in Fig.6. As it is obvious, experimental test and numerical simulation are in good agreement due to the negligible discrepancy between their results (less than 3%). Grippers' strain was neglected in numerical model as well as initial slid between sample and grippers, while they both affected the measured strain in experimental model. These simplifications may cause the mentioned negligible discrepancy between numerical and experimental models.
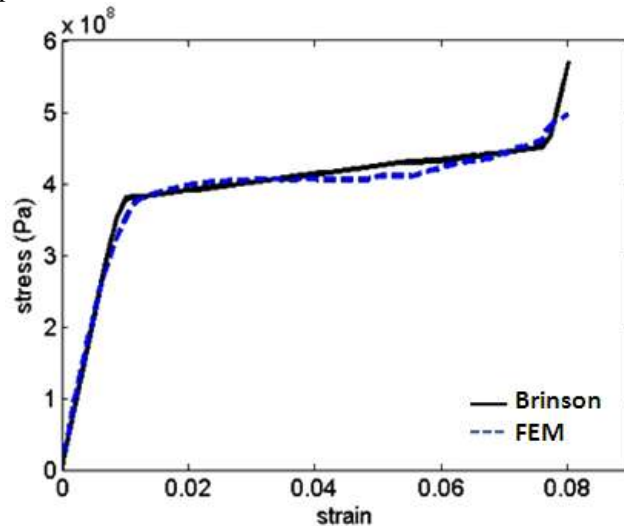

Fig.6. Nominal stress-Engineering strain in wire, FE and Brinson model

Fig. 7 depicts the stress pattern along the sample. As can be seen, stress pattern in a part of the sample located beneath the gripper is fully influenced by its presence; however, stress in this part of the sample was not taken into account in this study. Fig.7 shows that in contrast with remote sections from the gripper, such as section "A", sections located close to the gripper are locally affected by its presence (gripper-affected zone). The more the stress concentration increases in gripper-affected zone, the less the Brinson model could be accurate in predicting the stress pattern.
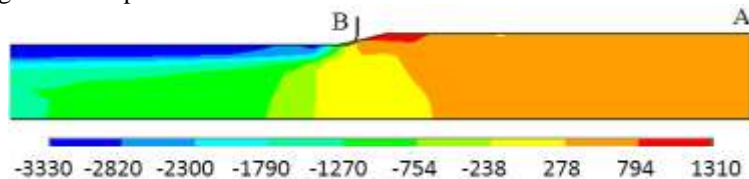

Fig.7. Stress pattern along the sample, FE model

Fig. 8 compares the stress variation on sample surface along the A-B line during the tension of the sample, extracted from FE and homogeneous Brinson model. Compare to the stress in sections remote from

gripper, containing a uniform stress distribution, stress increase at sections close to the gripper is obvious. As can be seen, Brinson stress is coincident with stress distribution extracted from FE model at sections located remote from the gripper. However, stress concentration causes a sudden increase in stress at gripper-affected zone which cannot be monitored by Brinson model. Therefore, the fundamental assumption of Brinson model, stress homogeneousness, causes a serious inaccuracy in predicting the stress and thus metallurgic phase at gripper-affected zone.
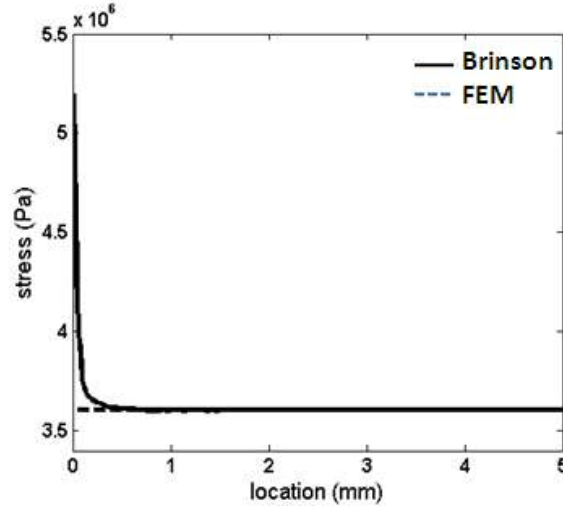

Fig.8. Stress variation along the A-B line, FE and homogeneous Brinson model

Comparing the stress pattern along the sample (Fig.8) with the given values of table1 shows that the substantial stress concentration in gripper-affected zone caused a considerable disturbance in stress homogeneousness and thus martensite volume fraction. Hence nucleation happened locally near the gripper while regions remote from the gripper were still in austenite phase. However, Brinson model estimated a homogeneous stress pattern and thus an austenite phase entire the sample.

III.   PROPOSED METHOD TO ENHANCE THE BRINSON MODEL

As mentioned before, an iterative algorithm is proposed in this research to enhance the Brinson model in which, maximum stress is taken into account instead of the mean stress. To do so, a code was developed to calculate the stress, strain and martensite volume fraction in various load cases based on the mentioned algorithm. Maximum stress due to some fractions of the final load, calculated in FE model at each section, was employed in the code and errors were eliminated in an iterative training procedure. An illustration of the algorithm flow chart is given in Fig.9.
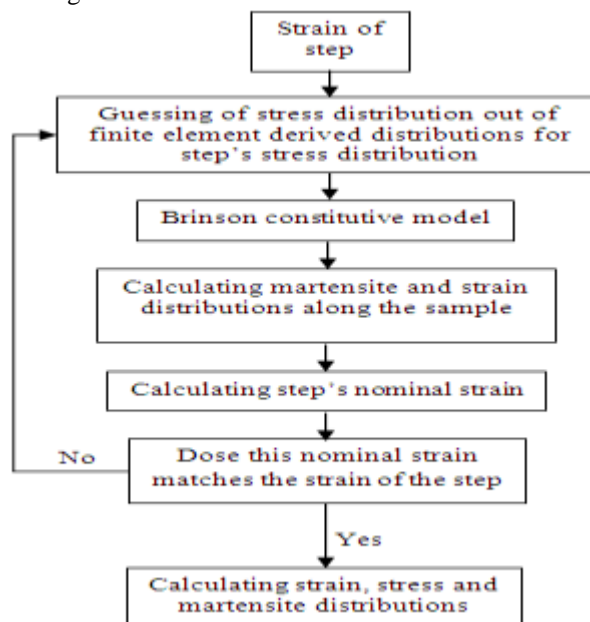

Fig.9. Flow chart of the algorithm proposed to enhance the Brinson model [19]

Initial stress pattern along the sample under a fraction of final displacement was calculated using FE model and were introduced to the proposed code. Brinson model was implemented to determine the martensite volume fraction and thus strain pattern at each section along the sample based on the FE stress in each step. Meanwhile the nominal strain was calculated. An error function was defined based on the discrepancy between calculated "Engineering strain" and "Resultant strain". Initial stress pattern was revised iteratively at each load step in case the error was higher than convergence criterion. This derived stress distribution would be considered as the initial guess for the next step.

In contrast with homogeneous Brinson model, real stress distribution was employed in this algorithm to calculate the martensite volume fractions and strains along the sample; hence peak stresses could be taken into account. Fig.10 depicts the nominal stress-strain curve along the sample predicted by FE model, proposed algorithm and homogeneous Brinson model.
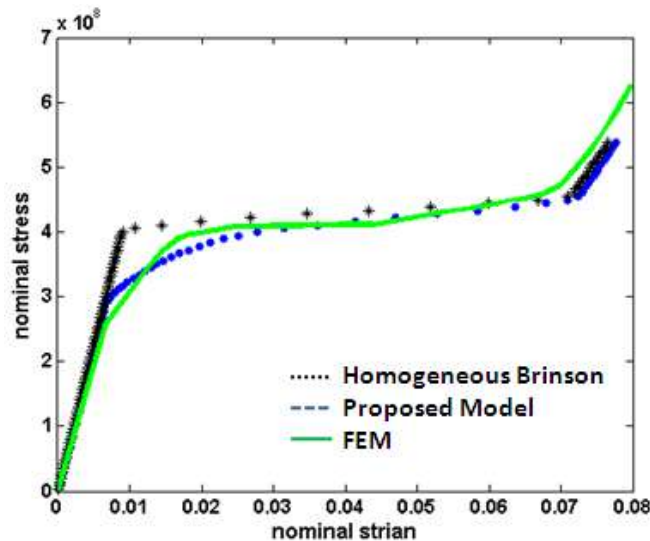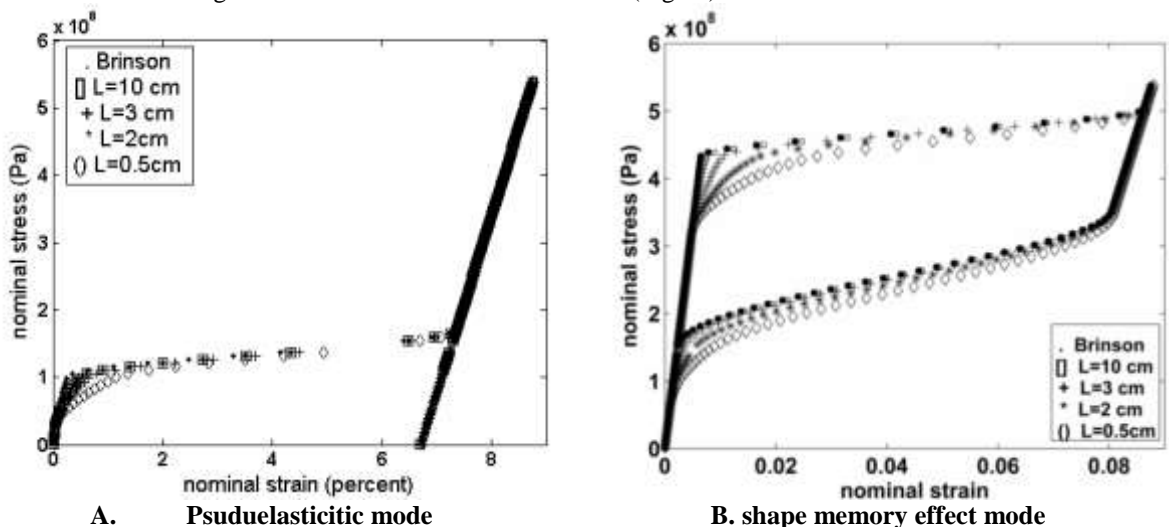

Fig.10. Nominal stress-strain curve

Compare to the homogeneous Brinson model, considering the stress concentration due to the gripper in the proposed algorithm leads to a considerable change in nominal stress-strain curve especially at the beginning of the plateau. Nucleation starts in elements located in gripper-affected zone before the nominal stress reaches the transformation start stress which leads to a increase in strain of elements and disfigure the stress-strain curve especially at the beginning of the plateau.

Nominal stress-strain curve of the wires with different length and diameters were calculated based on modified Brinson model to evaluate the generalization of proposed algorithm in psuduelasticity and shape memory effect modes. Fig.11 illustrates the stress-strain curves in wires with different length ranged from 5 to 100 mm, while the diameter of the wires remained constant, 1.5 mm. Furthermore, some 30 mm-long wires with different diameters ranged from 1 to 8 mm are also evaluated (Fig.12)

A. Psuduelasticitic mode	B. shape memory effect mode

Fig.11. Variation of nominal stress-strain curve with length of wires, with 1.5 mm diameter

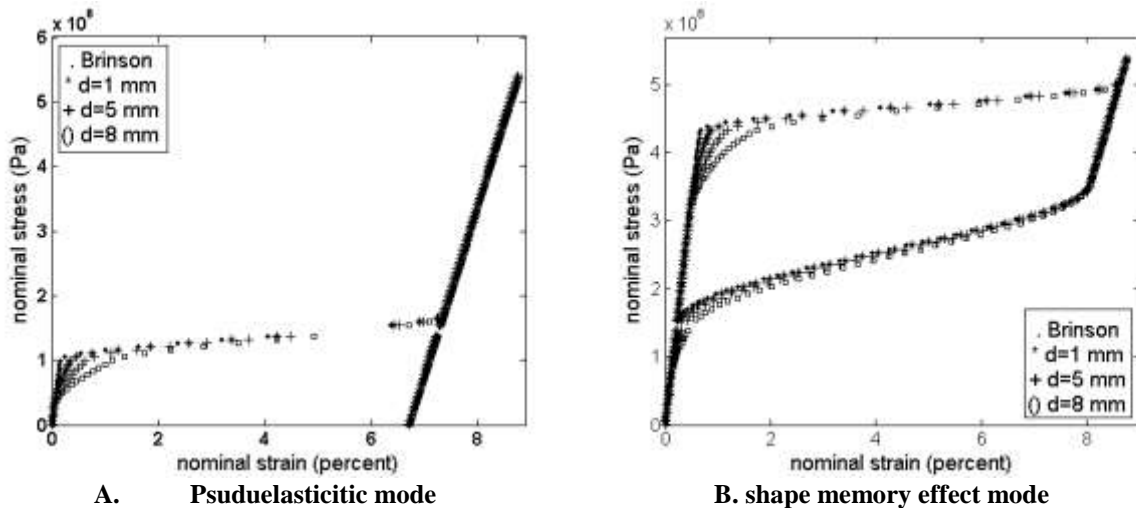**A. Psuduelasticitic mode**   **B. shape memory effect mode**

Fig.12. Variation of nominal stress-strain curve with diameter of wires, with 30 mm length

Obviously, the length of the span located away from the gripper-affected zone shrinks as the length of the wire decreases; hence stress predicted by homogeneous Brinson model will be more erroneous in case small wires are evaluated. Furthermore, the radial influence of gripper stress concentration rises as the wire diameter increases. Therefore, the ratio of nucleated to un-nucleated portion of the sample increases which leads to a higher bow in stress-strain curve especially at the beginning of the plateau.

Fig.11 reveals that the maximum stress discrepancy between homogeneous Brinson and proposed algorithm (almost 37%), modified Brinson model, occurs when a 5 mm-long wire with 1.5 mm diameter is implemented. However, this discrepancy reduces to 3% in case wires with 100 mm length and 1.5mm diameter is employed. Likewise, Fig.12 shows that maximum stress discrepancy between homogeneous and modified Brinson model (less than 24%) occurs in case a 30 mm-long wire with 8 mm diameter is implemented. This considerable difference reduces to 7% when a 30 mm-long wire with 1 mm diameter is employed. Figs.11 and 12 illustrate that the accuracy of the homogeneous Brinson model declines as the length of sample reduces, while the result of modified Brinson model remains acceptable. However, the modified and homogeneous Brinson results converge considerably when a long sample is investigated.

The martensite volume fraction distribution is evaluated along a 10 mm-long wire under tension to investigate the effect of stress concentration. Fig.13 depicts the changes in martensite volume fraction along the wire in some sequences of tensile loading. Fig.13 A illustrates that the stress concentration at near-gripper region initiates the nucleation which extends along the wire length as tension increases, whereas a constant martensite volume fraction is predicted by homogeneous Brinson model due to its incapability in predicting the stress pattern along the wire (Fig.13 B). Propagation of the transformation front at gripper-affected zone is clearly shown in Fig.13 A.
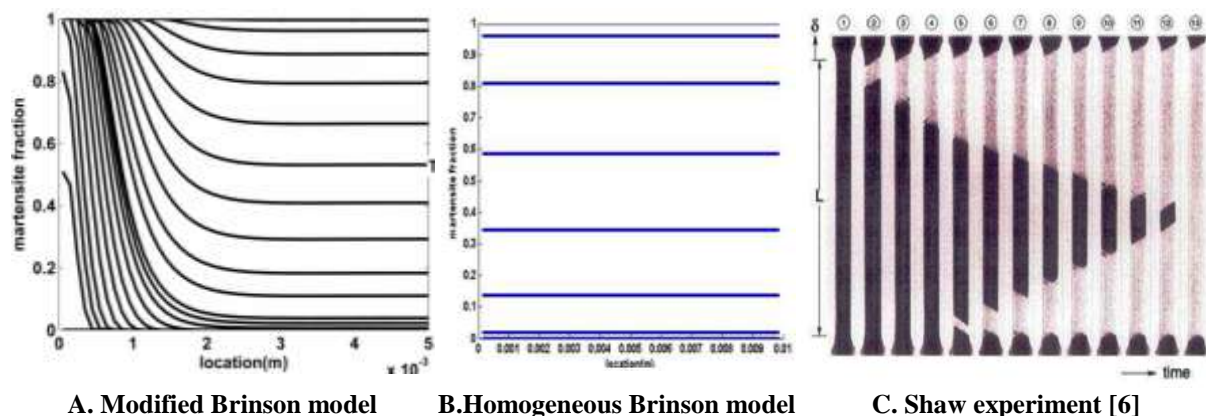

A. Modified Brinson model   **B.Homogeneous Brinson model**   **C. Shaw experiment [6]**

Fig.13. Martensite volume fraction distribution along the wire under tension

Shaw carried out an experiment in which the sample was coated using a brittle film. The brittle coat detached during the transformation and thus circumscribed the boundary of the nucleated zone (Fig.13 C). Fig.13 C shows a number of pictures of the samples under increasing tensile loads. As can be seen,

transformation started at one gripper-affected zone, followed by a transformation at the other gripper-affected zone and continued to extend towards the middle section of the wire.

Comparing the modified and homogeneous Brinson models with Shaw's experiments (Fig.13 A, B and C) reveals that modified Brinson model proposed in the present study not only could predict the stress and strain pattern precisely, but also is capable in accurately predicting the martensite volume fraction and thus material behavior.

IV. SUMMARY AND CONCLUSIONS

Implementation of a 1D, homogeneous Brinson model for the prediction of stress pattern and martensitic volume fraction distribution in a sample with stress concentration was investigated in this study. The proposed method begins by guessing an initial stress pattern in a small wire under tension based on the results of a FE analysis which would reveal the stress concentration in the gripper-affected zone. A code was developed to improve the accuracy of the Brinson model using FE data to iteratively modify the stress pattern considering stress concentration. The maximum stress in each section was substituted for the mean stress in the Brinson constitutive model. Evaluation of the results in gripper-affected zone showed a negligible discrepancy between stress distribution calculated by the developed code and FE analysis. Moreover, generalization assessments, performed by changing the length and diameter of the wire, revealed that the proposed code could accurately predict the stress distribution as well as martensitic volume fraction in both pseudo-elastic and shape memory effect modes. A case study showed that the modified model could improve the accuracy of the Brinson model by more than 36% in a 5mm long, 1.5mm thick wire.

REFERENCES

[1]. Auricchio, F., Taylor, R.L., Lubliner, J. Shape-memory alloys: macromodelling and numerical simulations of the superelastic behavior. Journal of Computer methods in applied mechanics and engineering, Vol.(146), pp. 281-312 (1997).

[2]. Tanaka, K. A thermo-mechanical sketch of Shape Memory Effect: One Dimensional Tensile Behavior. Res. Mech., Vol.(18), pp. 251-263 (1986).

[3]. Brinson, L.C. One-dimensional constitutive behavior of shape memory alloys: Thermo-mechanical derivation with Non-constant material functions and redefined martensie internal variable. Journal of intelligent material systems and structures, Vol.(4), pp. 1163-1181 (1993).

[4]. Brinson, L.C., Schmidt, I., Lammering, R. Stress-Induced transformation behavior of a polycrystalline NiTi shape memory alloy: Micro and macro-mechanical investigations via in situ optical microscopy. JMPS, Vol.(12), pp. 534-542 (2003).

[5]. Shaw, J.A., Kyriakides, S. Thermo-mechanical aspects of NiTi. J. Mech. Phys. Solids, Vol.(43), No. 8, pp. 1243-1281 (1995).

[6]. Shaw, J.A. Simulations of localized thermo-mechanical behavior in a NiTi shape memory alloy. International Journal of Plasticity, Vol.(16), pp. 541-562 (2000).

[7]. Rahman, M.A, Tani, j. Local Deformation Characteristics of the Shape Memory Alloy Rods during Forward and Reverse Stress Induced Martensitic Transformations. Journal of Intelligent Material Systems and Structures, Vol.(17), pp. 959-982 (2006).

[8]. Iadicola, M., Shaw, A. An experimental setup for measuring unstable thermo-mechanical behavior of shape memory alloy wire. Journal of intelligent material system and structures, Vol.(2), pp. 187-195 (2002).

[9]. Falk, F. Model Free Energy, Mechanics, and Thermodynamics of Shape Memory Alloys. Acta. Mtall., Vol.(28), pp. 1773-1780 (1980).

[10]. Muller, I., Huibin, X.U. On the Psudo-Elastic Hysteresis. Acta metal. Mater., Vol.(39), pp. 263-271 (1991).

[11]. Iadicola, M., Shaw, A. Rate and thermal sensitivities of unstable transformation behavior in a shape memory alloy. International Journal of Plasticity, Vol.(20), pp. 577-605 (2004).

[12]. Azadi, B., Rajapakse, R.K.N.D., Maijer, D.M. One-dimensional thermo-mechanical model for dynamic pseudo-elastic response of shape memory alloys. J. Smart Mater. Struct. Vol.(15), pp. 996–1008 (2006).

[13]. Duval, A., Haboussi, M., Zineb, T.B. Modeling of SMA super-elastic behavior with nonlocal approach. 3rd International Symposium on Shape Memory Materials for Smart Systems, France, 2010

[14]. Duval, A., Haboussi, M., Zineb, B. Modeling of localization and propagation of phase transformation in super-elastic SMA by a gradient nonlocal approach. International Journal of Solids and Structures, Vol.(48), pp. 1879–1893 (2011).

[15]. Zhang, X., Feng, P.,He, Y.,Yu, T., Sun,Q. Experimental study on rate dependence of macros copic domain and stress hysteresis in NiTi shape memory alloy strips. International Journal of Mechanical Sciences, Vol.(52), pp. 1660 –1670 (2010).

[16]. Spies, R.D. An algorithm for simulating the isothermal hysteresis in the stress-strain laws of shape memory alloys. Journal of Materials Science, Vol.(31), pp. 6631-6636 (1996).

[17]. Okabe, N., Hosogi, M., Sakuma, T., Okita, K. A New Fatigue Model for Titanium-Nickel-Copper Shape Memory Alloy Subjected to Superelastic Cyclic Deformation. MATERIALS TRANSACTIONS, Vol.,(43), pp. 809-814 (2002).

[18]. Kim, Y. Fatigue Properties of the Ti-Ni Base Shape Memory Alloy Wire. MATERIALS TRANSACTIONS, Vol.(43), pp. 1703-1706 (2002).

[19]. Kamrani, M., Kadkhodaei, M. Investigation into the Simple Tensile Test of SMA Wires Considering Stress Concentration of Grippers. Proceedings of Journal of Materials Engineering and Performance, JMEP-13-07-4982 (2013).